RESEARCH MEMORANDUM

EFFECT OF FUSELAGE CIRCUMFERENTIAL INLET LOCATION ON DIFFUSER-DISCHARGE TOTAL-PRESSURE PROFILES AT SUPERSONIC SPEEDS

By Emil J. Kremzier and Joseph F. Wasserbauer

Lewis Flight Propulsion Laboratory
Cleveland, Ohio

NATIONAL ADVISORY COMMITTEE FOR AERONAUTICS

WASHINGTON

October 29, 1956

NACA RM E56G26

NATIONAL ADVISORY COMMITTEE FOR AERONAUTICS

RESEARCH MEMORANDUM

EFFECT OF FUSELAGE CIRCUMFERENTIAL INLET LOCATION ON DIFFUSER-DISCHARGE TOTAL-PRESSURE PROFILES AT SUPERSONIC SPEEDS

By Emil J. Kremzier and Joseph F. Wasserbauer

SUMMARY

An investigation of the effect of fuselage circumferential inlet location on diffuser-discharge total-pressure profiles was conducted in the Lewis 8- by 6-foot supersonic wind tunnel over a range of inlet corrected air flows for angles of attack up to 9°. The least change with angle of attack in both total-pressure contours and total-pressure distortion at the diffuser discharge was observed for the inlet located on the bottom of the fuselage. The greatest change in distortion level with angle of attack was obtained for the side-inlet location. The magnitude of this change could be reduced somewhat by reorientation of the ramp surface to give increased compression at angle of attack. Variation in distortion level for the top-inlet configurations with angle of attack was largely confined to the supercritical range of inlet operation. Addition of fuselage fences ahead of the top inlet was effective at moderate angles of attack in preventing some of the low-energy air associated with the body crossflow field from entering the inlet.

INTRODUCTION

Some of the effects of inlet location on the performance of inlets mounted on a fuselage are reported in references 1 to 3. Variations in the flow field with circumferential position on a fuselage at angle of attack result in large variations in inlet pressure recovery and drag. The investigation of reference 1 points out that the pressure recovery and drag of a bottom inlet are higher than those for a top inlet at angle of attack. Also, the addition of fuselage fences improves the angle-of-attack pressure recovery of a top inlet at the expense of some increase in drag. Reference 2 shows that it is possible to improve the pressure recovery of a side inlet at moderate angles of attack (free-stream Mach number of 2.0) by a reorientation of the external compression surface to give increasing compression with increasing angle of attack.

While the variations of inlet pressure recovery and drag are important factors in the evaluation of the performance of a propulsion system, the distortion and distribution of total pressure at the diffuser discharge are also important considerations. Flow distortions in the air-induction system can reduce the surge margin of turbojet compressors, thereby reducing engine acceleration and altitude operating capabilities. In addition, local increases in turbine gas temperature may occur, requiring an engine thrust derating as a protective measure. Other undesirable effects such as rotating stall and increased compressor blade vibratory stresses can also exist. Some of the factors influencing the amount of flow distortion encountered in air-induction systems are discussed in references 4 to 6.

The present investigation is an extension of the information contained in references 1 and 2 to include the effects of inlet location on diffuser-discharge total-pressure profiles. Top, side, and bottom inlet locations on the NACA RM-10 body of revolution are considered. Most of the data presented are for a free-stream Mach number of 2.0 and for a range of angle of attack and inlet corrected weight flow.

SYMBOLS

P_{av}	average area-weighted total pressure at diffuser discharge
P_{max}	maximum local total pressure at diffuser discharge
$\frac{P_{max} - P_{min}}{P_{av}}$	flow-distortion parameter
P_{min}	minimum local total pressure at diffuser discharge within 95 percent of duct radius
P_0	free-stream total pressure
P_3	local total pressure in duct at diffuser discharge
$\frac{w\sqrt{\theta}}{\delta A}$	corrected weight flow per unit area at diffuser discharge, (lb/sec)/sq ft
α	model angle of attack

[redacted]

APPARATUS AND PROCEDURE

The data presented in this report were obtained from the investigations reported in references 1 and 2, which include detailed descriptions of the models and instrumentation. A schematic drawing of the models discussed herein is presented in figure 1. Configuration A utilized a conventional ramp-type inlet with the ramp surface curved parallel to the fuselage surface and separated from the fuselage by a wedge-type boundary-layer diverter. The inlet was positioned successively on the top, side, and bottom of the fuselage. The inlet of configuration B was mounted only on the side of the fuselage with a flat ramp surface perpendicular to the fuselage surface. The ramp surface was located across the top of the duct and imparted a downward deflection to the inlet air. The inlet for this configuration was also separated from the fuselage by a boundary-layer diverter and included side fairings on the ramp to minimize flow spillage from the compression surface.

Diffuser-discharge total pressures were determined with a total-pressure rake located at model station 66.5 just downstream of the diffuser discharge. The flow-distortion parameter $(P_{max} - P_{min})/P_{av}$ was obtained from the difference between the maximum and minimum total pressures at the diffuser discharge within 95 percent of the duct radius divided by the average total pressure.

The investigation was conducted in the NACA Lewis 8- by 6-foot supersonic wind tunnel over a range of inlet corrected weight flows and at angles of attack of 0°, 3°, 6°, and 9°. Most of the data presented were obtained at a free-stream Mach number of 2.0. Reynolds number range for the investigation was from 26.9×10^6 to 33.0×10^6 based on model length.

RESULTS AND DISCUSSION

Contours of the local total-pressure recovery at the diffuser discharge for configuration A are presented in figures 2(a), (b), (c), and (d) for the bottom inlet, side inlet, top inlet, and top inlet with fences, respectively. All contours are presented for the inlet at or near critical operation. Little change in the position of the high-energy core with increasing angle of attack is noted for the bottom inlet (fig. 2(a)). At an angle of attack α of 9°, however, this core spreads out, covering a larger portion of the duct, and the separated region, indicated by the shaded area at the top of the duct, disappears. The separation at the top of the duct at the lower angles of attack is probably a result of ramp surface shock - boundary-layer interaction together with failure of the flow to follow the ramp surface curvature. At $\alpha = 9^\circ$, the strength of the terminal shock on the ramp surface is reduced because of the compression of the flow on the bottom of the fuselage,

[redacted]

which reduces the Mach number ahead of the inlet. The ramp surface pressure is also increased, which tends to increase the spillage of the boundary layer off the edges of the ramp. Thus, the magnitude of the shock - boundary-layer interaction is reduced.

For the side inlet (fig. 2(b)), the high-energy core at zero angle of attack is located in the right half of the duct, the separated region again occurring on the ramp side at the left. At angle of attack, the high-energy core moves into the upper right quandrant, and the separation moves down into the lower left quandrant. Although the local Mach number and crossflow angle of attack at the inlet increase with model angle of attack, no appreciable change in the amount of separation is noted.

The high-energy core in the contours for the top inlet (fig. 2(c)) does not change position with increasing angle of attack up to 6°. The region of separation increases, however, probably as a result of boundary-layer thickening on the leeward side of the body, as illustrated in the Pitot pressure contours of reference 3 at body station 45. These contours show a general thickening of the low-energy air region at the top of the body with increasing angle of attack up to about 6°. Above 6°, the contours indicate the formation of a vortex system in this region which tends to sweep away the low-energy air near the top surface of the body at the base of the inlet. This reduction in the amount of low-energy air at the inlet ramp surface reduces the inlet shock - boundary-layer interaction to such a large extent that no separation is observed in the diffuser-discharge total-pressure contours at 9° angle of attack. It is also apparent that the crossflow vortex system imparts a downward component to the flow velocity near the center of the inlet, resulting in a downward displacement of the high-energy core at the diffuser discharge for 9° angle of attack. It is quite probable that some of the low-energy air from the vortex system enters the inlet, since the pressure level of the contours at 9° is lower than that for the lower angles of attack.

The addition of body fences to the top-inlet configuration (fig. 2(d)) has no noticeable effect on the variation in position of the high-energy core at the diffuser discharge with angle of attack. No increase in the amount of separation with increasing angle of attack up to 6° is noted, however, indicating effective blocking of the body crossflow by the fences. At 9° angle of attack, the crossflow vortex system apparently is extensive enough to overcome the blocking effect of the fences, since the high-energy core is again displaced downward as for the top inlet without fences.

The total-pressure-ratio contours at the diffuser discharge for the side inlets of configurations A and B are compared in figure 3. The variation of the flow pattern of configuration A with angle of attack has already been discussed (fig. 2(b)). Reorientation of the ramp surface to the top of the duct for increased compression at angle of attack

results in the flow pattern shown in figure 3 for configuration B. The high-energy core of the total-pressure contours for this configuration shows very little change in position with increasing angle of attack. In reference 2, the pressure recovery of configuration B (horizontal ramp) was higher than that of configuration A (vertical ramp) over the angle-of-attack range at Mach 2.0. Despite this higher pressure recovery, a fairly extensive separated region can be observed on the ramp side of the duct, probably because of the presence of inlet side fairings that prevent ramp surface boundary-layer spillage off the edges of the ramp.

4118

Distortion levels $(P_{max} - P_{min})/P_{av}$ for the inlets of configurations A and B are presented in figures 4 to 6 as a function of diffuser-discharge corrected weight flow per unit area.

In figure 4, comparison of the distortion levels of the various inlets of configuration A indicates that the bottom inlet, top inlet, and top inlet with fences show the least variation with angle of attack in the vicinity of critical inlet operation. The general level of distortion for all of the inlets increases gradually with increasing air flow in the subcritical range, and increases more rapidly during supercritical operation. This trend is also observed in reference 4. The dashed curves for fully developed turbulent pipe flow are included for comparison.

The most pronounced effect of angle of attack on distortion is experienced with the side inlet (fig. 4(b)), where the effective angle of attack of the inlet is increased by the body crossflow.

The differences in distortion level with angle of attack for the top inlet with and without fuselage fences (figs. 4(d) and (c)) are largely confined to the supercritical range of inlet operation. These differences are not particularly significant, however, since the design operation of most inlets is generally in the vicinity of critical.

Figure 5 compares the distortion levels of the side inlet of configuration A at free-stream Mach numbers of 1.5 and 2.0. Data were available only for 0° and 6° angle of attack at Mach 1.5, but no significant change in distortion level with angle of attack is noted for this range. Also, the increase in distortion level with inlet corrected air flow is steady over the air-flow range, with no evidence of a pronounced increase in slope between subcritical and supercritical inlet operation. Since the ramp angle for this inlet exceeds the oblique-shock detachment angle at Mach 1.5, no strong terminal shock is formed on the ramp surface during subcritical inlet operation. In the supercritical range, a terminal shock forms in the subsonic diffuser, gradually moving downstream and increasing in strength as the inlet air-flow rate is increased. This gradual increase in shock - boundary-layer interaction results in a

[redacted]

smooth variation of distortion level with increasing air-flow rate, rather than the abrupt change that takes place when a strong terminal shock enters the inlet. The initial distortion level for critical inlet operation at zero angle of attack is higher at Mach 1.5 than at Mach 2.0, probably because of a greater flow velocity gradient across the inlet resulting from the detached bow wave formed by the large ramp angle.

The distortion levels for the side inlet of configurations A and B are compared in figure 6 for a free-stream Mach number of 2.0. The general trends of the variation of distortion with air-flow rate and angle of attack for the two inlets are similar. Configuration B, however, exhibits slightly less distortion increase with angle of attack at critical inlet operation. Thus, it appears that the adverse effects of angle of attack on the flow distortion of a side inlet can be reduced by orienting the ramp to give increased compression with increasing angle of attack.

SUMMARY OF RESULTS

The effect of fuselage circumferential inlet location on diffuser-discharge total-pressure profiles was investigated at supersonic speeds for a range of model angles of attack and inlet air-flow rates. The following results were obtained:

1. The flow conditions at the diffuser exit of the bottom inlet were least affected by changes in angle of attack. Both total-pressure contours and total-pressure distortion exhibited very little change with increasing angle of attack in the range from 0° to 9°.

2. Total-pressure distortion level for the side inlet showed the greatest increase with angle of attack and some change in position of the total-pressure contours. Reorientation of the inlet ramp surface to give increased compression at angle of attack effected a slight reduction of the distortion increase with angle of attack, while the reoriented total-pressure contours showed no significant change.

3. Variations in the distortion level with angle of attack at the diffuser discharge of the top-inlet configuration, while subject to total-pressure variations at the inlet associated with the body crossflow field, are largely confined to the supercritical range of inlet operation. Diffuser-discharge total-pressure contours indicate that the addition of fuselage fences ahead of the inlet is effective in preventing some of the low-energy air in the body crossflow field from entering the inlet at moderate angles of attack.

Lewis Flight Propulsion Laboratory
National Advisory Committee for Aeronautics
Cleveland, Ohio, July 27, 1956

[redacted]

REFERENCES

1. Kremzier, Emil J., and Campbell, Robert C.: Effect of Fuselage Fences on the Angle-of-Attack Supersonic Performance of a Top-Inlet - Fuselage Configuration. NACA RM E54J04, 1955.

2. Wise, G. A., and Campbell, R. C.: Investigation of a Ramp-Type Inlet Designed for Improved Angle-of-Attack Performance at Mach Number 2.0. NACA RM E54L17, 1955.

3. Valerino, Alfred S., Pennington, Donald B., and Vargo, Donald J.: Effect of Circumferential Location on Angle of Attack Performance of Twin Half-Conical Scoop-Type Inlets Mounted Symmetrically on the RM-10 Body of Revolution. NACA RM E53G09, 1953.

4. Piercy, Thomas G., and Klann, John L.: Experimental Investigation of Methods of Improving Diffuser-Exit Total-Pressure Profiles for a Side-Inlet Model at Mach Number 3.05. NACA RM E55F24, 1955.

5. Sterbentz, William H.: Factors Controlling Air-Inlet Flow Distortions. NACA RM E56A30, 1956.

6. Piercy, Thomas G.: Factors Affecting Flow Distortions Produced by Supersonic Inlets. NACA RM E55L19, 1956.

4118

[redacted]

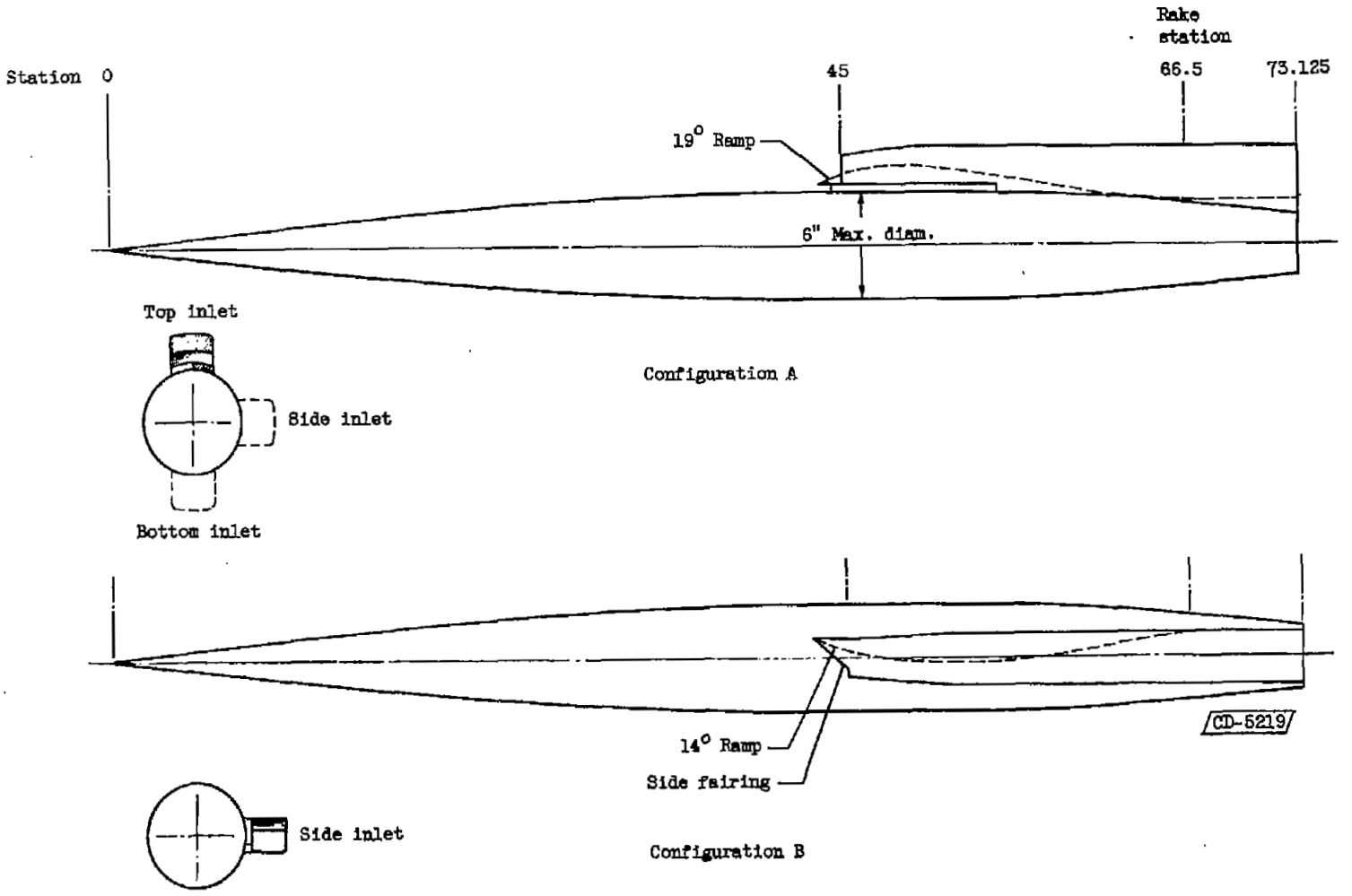

Figure 1. - Schematic drawing of models (dimensions in inches).

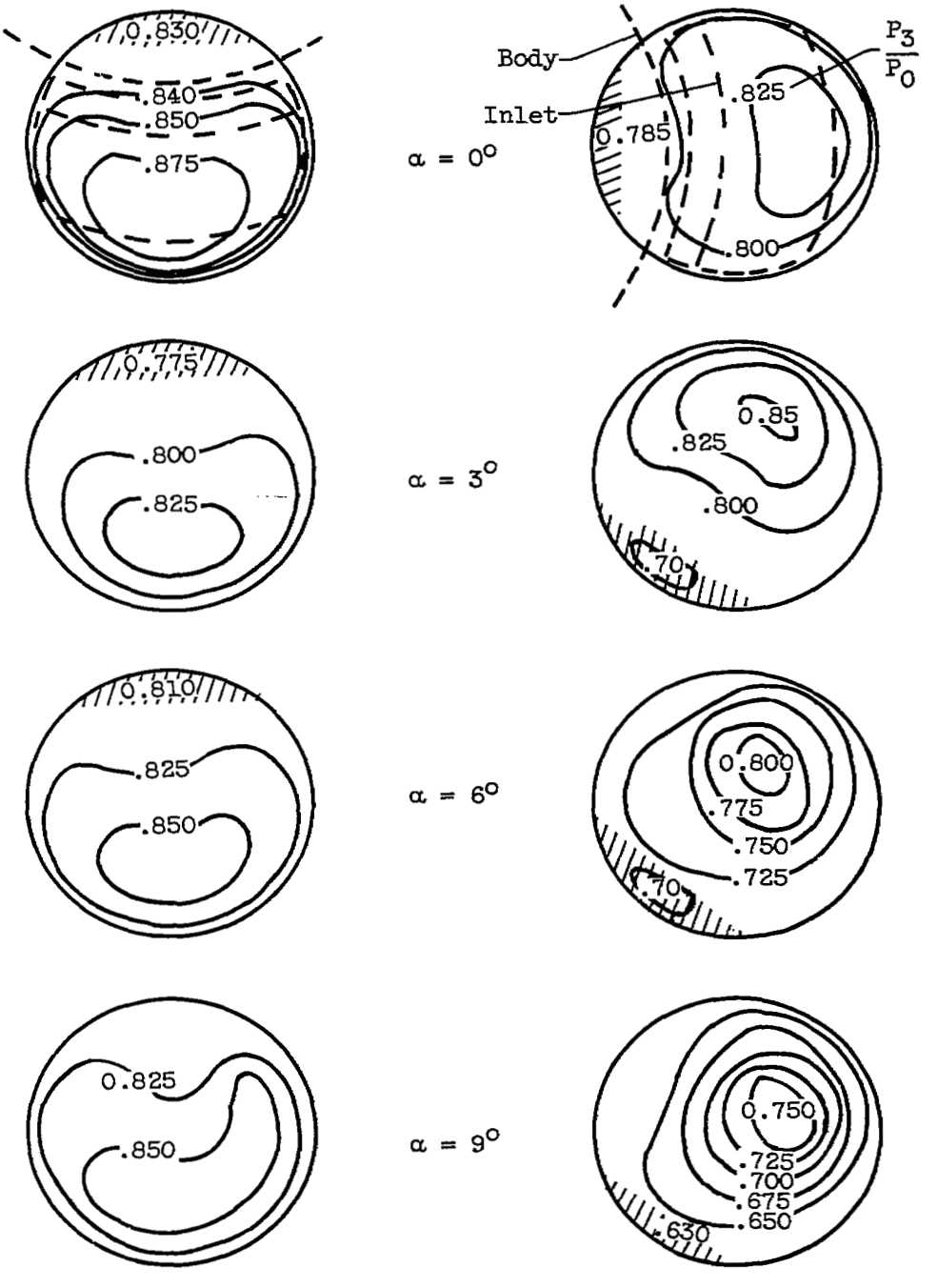

(a) Bottom inlet. (b) Side inlet.

Figure 2. - Total-pressure contours for configuration A at critical conditions. Free-stream Mach number, 2.0.

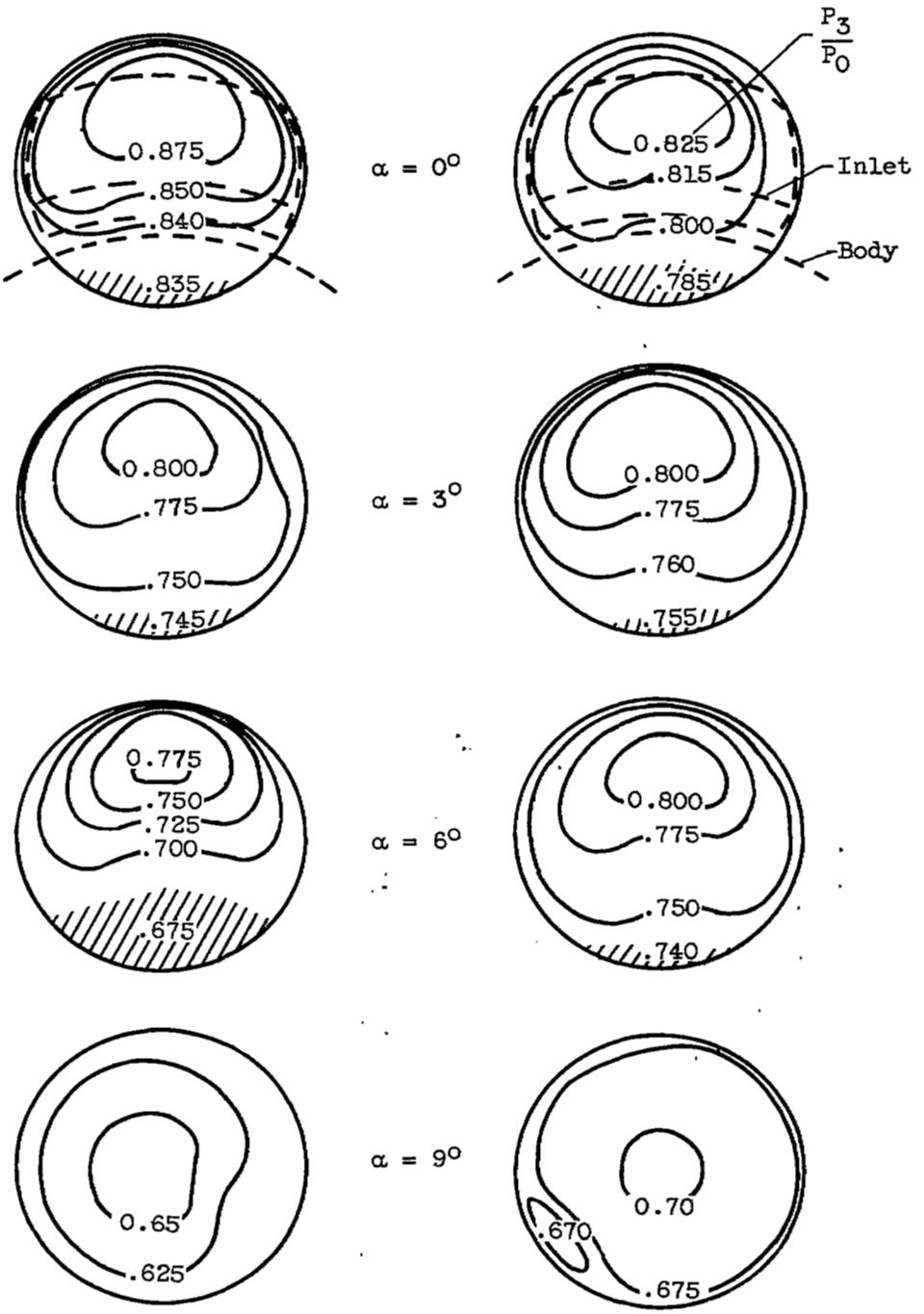

(c) Top inlet.

(d) Top inlet with fences.

Figure 2. - Concluded. Total-pressure contours for configuration A at critical conditions. Free-stream Mach number, 2.0.

[redacted]

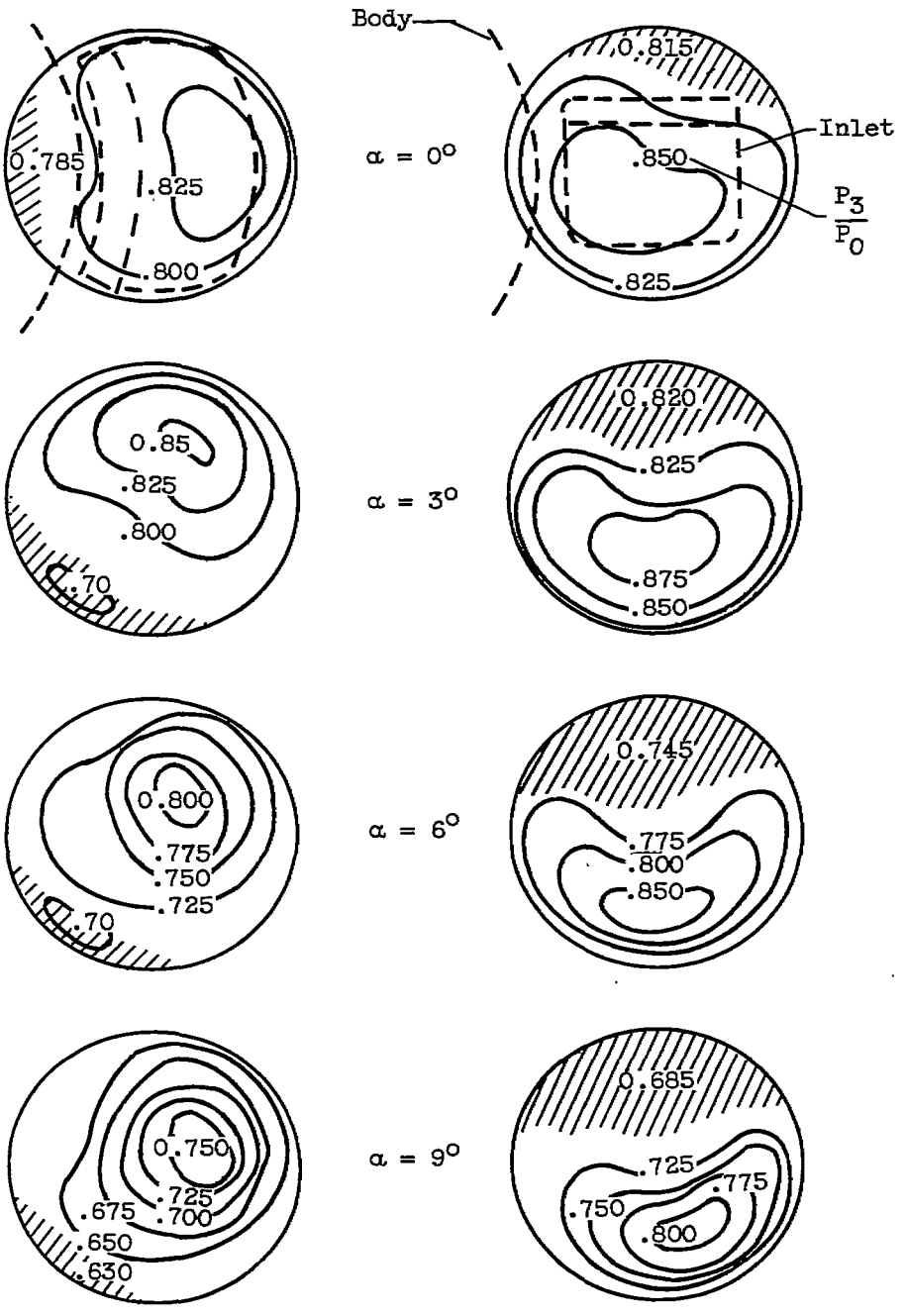

Configuration A Configuration B

Figure 3. - Comparison of contour plots at critical operation for side-inlet configurations A and B. Free-stream Mach number, 2.0.

[redacted]

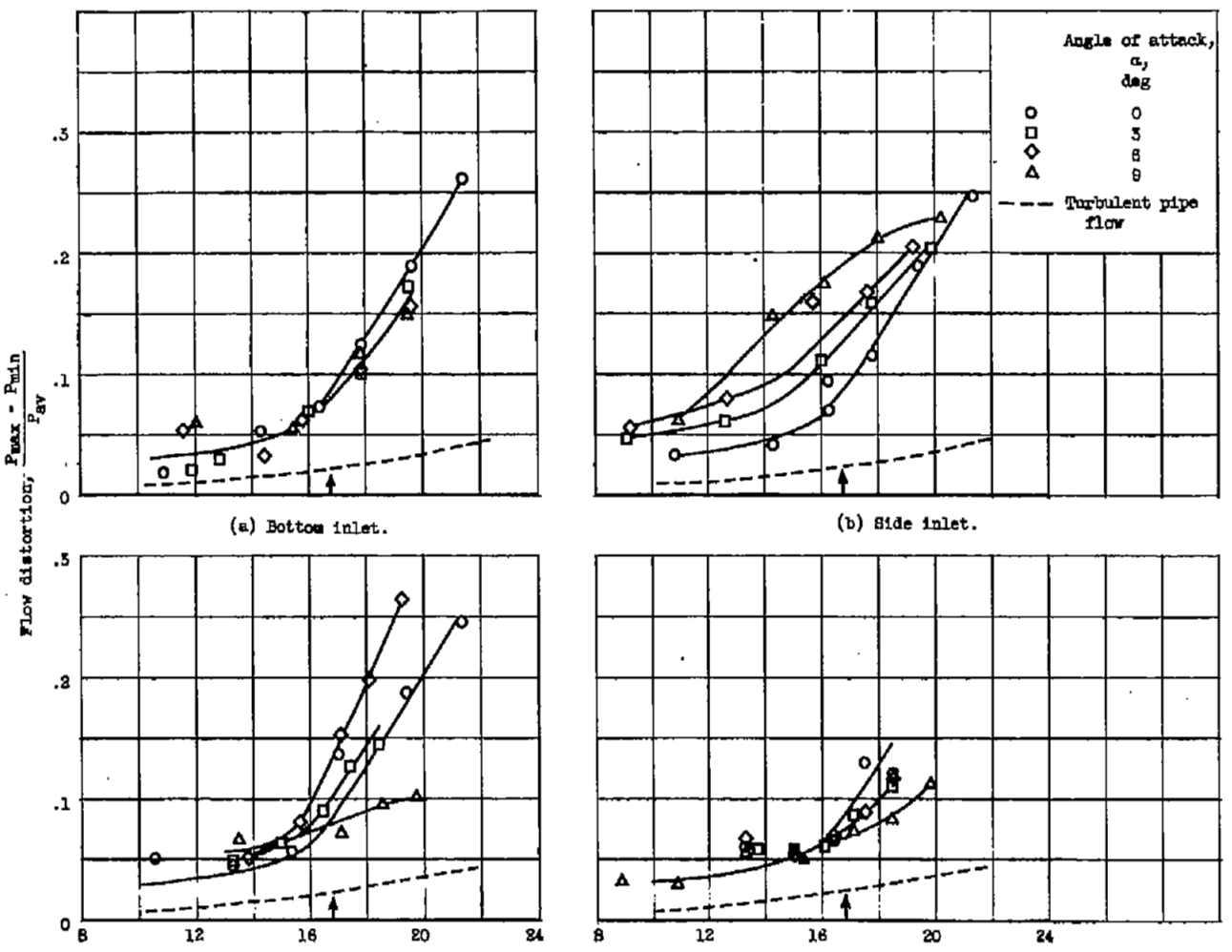

(a) Bottom inlet.

(b) Side inlet.

(c) Top inlet.

(d) Top inlet with fences.

Figure 4. - Distortion level for inlets of configuration A. Free-stream Mach number, 2.0. (Arrows indicate critical operation at zero angle of attack.)

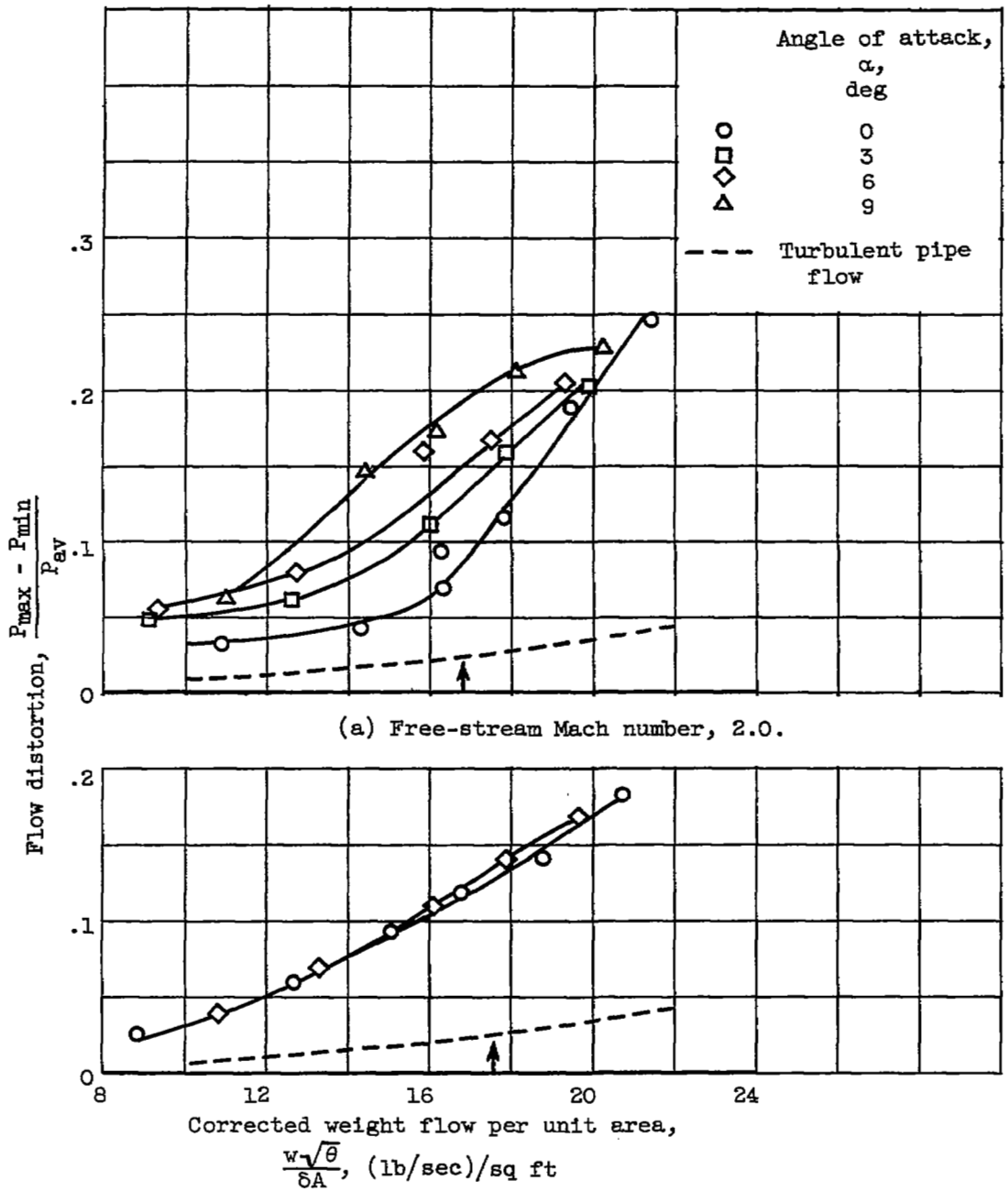

(a) Free-stream Mach number, 2.0.

(b) Free-stream Mach number, 1.5.

Figure 5. - Distortion level for side inlets of configuration A. (Arrows indicate critical operation at zero angle of attack.)

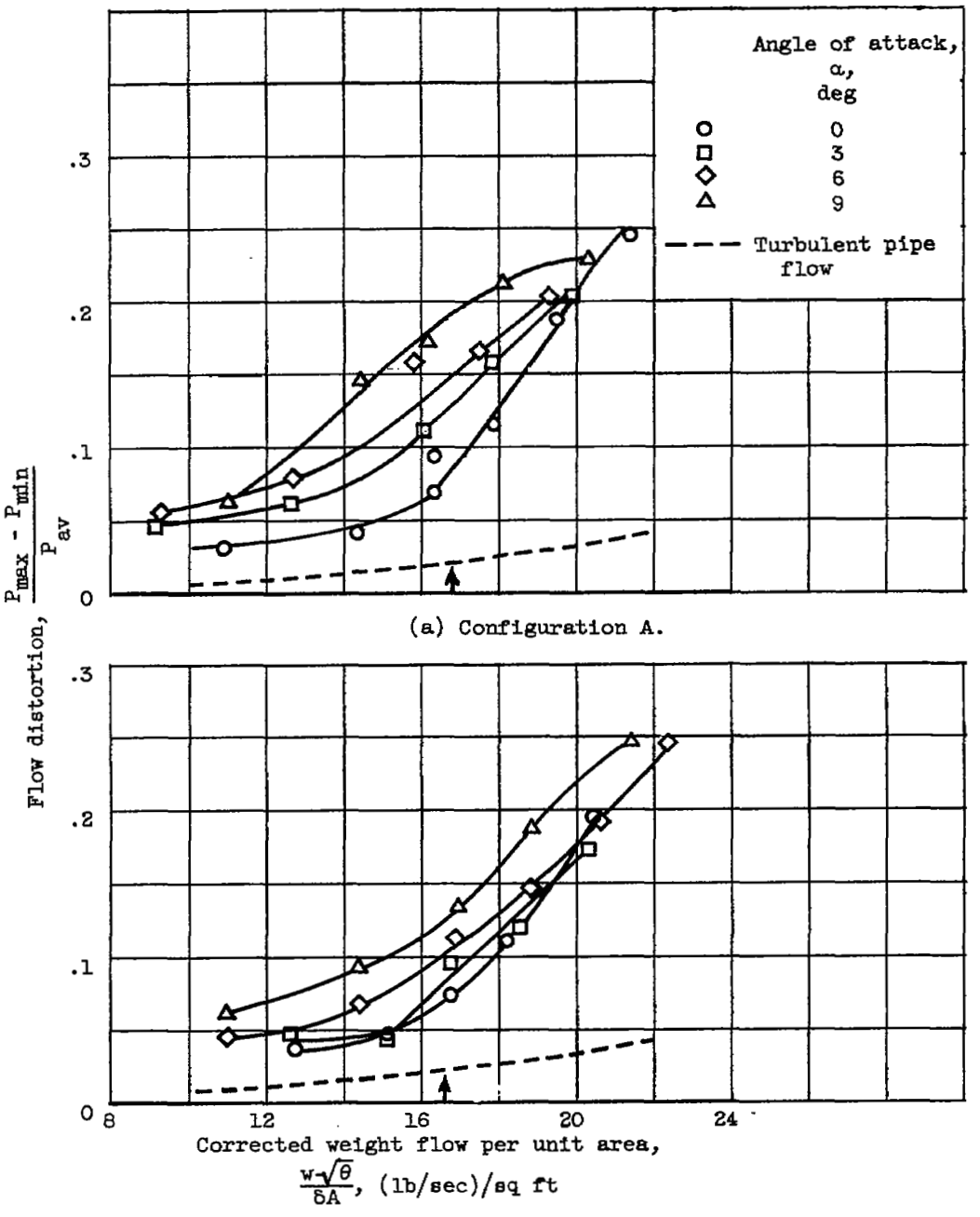

(a) Configuration A.

(b) Configuration B.

Figure 6. - Comparison of distortion level for side inlets of configurations A and B. Free-stream Mach number, 2.0. (Arrows indicate critical operation at zero angle of attack.)

[redacted]